Signal Period Analysis Based on Hilbert-Huang Transform and Its Application to Texture Analysis *

Zhihua Yang[1], Dongxu Qi[2] and Lihua Yang[3] †

[1]School of Information Science and Technology
Sun Yat-sen University, Guangzhou 510275, P. R. China

[2] Faculty of Information Technology
Macao University of Science and Technology, Macao

[3]School of Mathematics and Computing Science
Sun Yat-sen University, Guangzhou 510275, P. R. China

Abstract

An approach to analyze the period of a signal based on Hilbert-Huang Transform is presented in this paper. For an approximately periodic signal which contains plenty of high frequency components, the relation between its period and its main frequency is established. Our main result is that, for an approximately periodic signal which contains plenty of high frequency components, its period can be estimated accurately according to its main-frequency distribution. By applying the technique on texture analysis, a novel method to extract the perodicity features of a texture image is developed, which can be used in texture classification, segmentation, recognition and other applications.

Keywords: Empirical mode decomposition(EMD), Hilbert-Huang Transform(HHT), Texture analysis

1 Introduction

Hilbert-Huang Transform (HHT) is a novel analysis method for nonlinear and non-stationary data, which was developed by Huang et al [5] in 1998. Its key part is the so-called *empirical*

*This work was supported by NSFC(No. 60133020, 69873001), the National 973 Program (No. G1998030607), GDSF (No. 036608) and the foundation of scientific and technological planning project of Guangzhou city (No. 2003J1-C0201).

†Corresponding author. Email: mcsylh@zsu.edu.cn, Tel: (8620)84115508, Fax: (8620)84111696.

mode decomposition (EMD), with which any complicated data set can be decomposed into finite (often less) number of *intrinsic mode functions (IMFs)* which admit well-behaved Hilbert transforms. With Hilbert transform, the IMFs yield instantaneous frequencies as functions of time, that give sharp identifications of imbeded structures. The final presentation of the results is a time-frequency-energy distribution, designated as the Hilbert spectrum. Being different from Fourier decomposition and wavelet decomposition, EMD has no specified "basis". Its "basis" is adaptively produced depending on the signal itself, which brings not only high decomposition efficiency but also sharp frequency and time localization. A key point is that the signal analysis based on HHT is physically significant. Because of its excellence, HHT has been utilized and studied widely by researchers and experts in signal processing and other related fields. In recent years, more and more works on HHT theory and application are reported such as [3, 2]. Its application on the signal analysis have spread from earthquake research [9], ocean science [6], biomedicine [7, 8, 15, 12], speech signal analysis [14] to image analysis and processing [4]. In 2003, J. C. Nunes et al extended EMD method from one-dimension to two dimension and developed a decomposition algorithm for two dimension data, which is called Bidimensional Empirical Mode Deposition (BEMD), and was used to extract texture features at multiple scales or spatial frequencies [11, 10] and other applications.

Period analysis based on HHT is introduced in this paper. For an approximately periodic signal containing rich high frequency components, the relation between its period and its main frequencies is found by analyzing the influence of the signal's non-linearity on the distribution of the main frequency. It is used to estimate the period according to the main frequency distribution (MFD) of a signal in this paper and our experiments show positive results. Once it is applied into the analysis of natural texture image, the period characteristic of the texture image can be extracted, which provides the new approach to texture classification, segment, recognition and image index.

The rest of the paper is organized as follows: Section 2 is a brief summary of Hilbert-Huang Transform; Analysis of signal period based on HHT is given in Section 3; In Section 4, the theory presented in Section 3 is used to analyzing textures and experiments are conducted to support our results; Finally, Section 5 is the conclusion of this paper.

2 Hilbert-Huang Transform

Hilbert-Huang Transform (HHT) was proposed by Huang et al [5]. It consists of two parts: (1) *Empirical Mode Decomposition (EMD)*, and (2) *Hilbert Spectral Analysis*. With EMD, any complicated data set can be decomposed into a finite and often less number of *intrinsic mode functions (IMFs)*. An IMF is defined as a function satisfying the following conditions:

(a) The number of extrema and the number of zero-crossings must either equal or differ at most by one;

(b) At any point, the mean value of the envelope defined by the local maxima and the envelope defined by the local minima is zero.

An IMF defined as above admits well-behaved Hilbert transforms. EMD decomposes signals adaptively and is applicable to nonlinear and non-stationary data (Fundamental theory on nonlinear time series can be found in [1]). In this section, a brief introduction is given to make this paper somewhat self-contained. The readers are referred to [5] for details.

For an arbitrary function, $X(t)$, in Lp-class [13], its Hilbert transform, $Y(t)$, is defined as

$$Y(t) = \frac{1}{\pi} P \int_{-\infty}^{\infty} \frac{X(t')}{t - t'} \mathrm{d}t', \tag{2.1}$$

where P indicates the Cauchy principal value. Consequently an analytic signal, $Z(t)$, can be produced by

$$Z(t) = X(t) + iY(t) = a(t)e^{i\theta(t)}, \tag{2.2}$$

where

$$a(t) = [X^2(t) + Y^2(t)]^{\frac{1}{2}}, \quad \theta(t) = \arctan(\frac{Y(t)}{X(t)}) \tag{2.3}$$

are the instantaneous amplitude and phase of $X(t)$.

Since Hilbert transform $Y(t)$ is defined as the convolution of $X(t)$ and $1/t$ by Eq. (2.1), it emphasizes the local properties of $X(t)$ even though the transform is global. In Eq. (2.2), the polar coordinate expression further clarifies the local nature of this representation. With Eq. (2.2), the instantaneous frequency of $X(t)$ is defined as

$$\omega(t) = \frac{d\theta(t)}{dt}. \tag{2.4}$$

However, there is still considerable controversy on this definition. A detailed discussion and justification can be found in [5].

EMD is a necessary pre-processing of the data before the Hilbert transform is applied. It reduces the data into a collection of IMFs and each IMF, which represents a simple oscillatory mode, is a counterpart to a simple harmonic function, but is much more general. We will not describe EMD algorithm here due to the limitation of the length of the paper. The readers are referred to [5] for details.

By EMD, any signal $X(t)$ can be decomposed into finite IMFs, $\mathrm{imf}_j(t)$ $(j = 1, \cdots, n)$, and a residue $r(t)$, where n is nonnegative integer depending on $X(t)$, i.e.,

$$X(t) = \sum_{j=1}^{n} \mathrm{imf}_j(t) + r(t). \tag{2.5}$$

For each $\mathrm{imf}_j(t)$, Let $X_j(t) = \mathrm{imf}_j(t)$, its corresponding instantaneous amplitude, $a_j(t)$, and instantaneous frequency, $\omega_j(t)$, can be computed with Eqs. (2.3) and (2.4). By Eqs.

(2.2) and (2.4), $\mathrm{imf}_j(t)$ can be expressed as the real part, RP, in the following form:

$$\mathrm{imf}_j(t) = RP\left[a_j(t)\exp\left(i\int \omega_j(t)dt\right)\right]. \tag{2.6}$$

Therefore, by Eqs. (2.5) and (2.6), $X(t)$ can be expressed as the IMF expansion as follows:

$$X(t) = RP\sum_{j=1}^{n} a_j(t)\exp\left(i\int \omega_j(t)dt\right) + r(t), \tag{2.7}$$

which generalize the following Fourier expansion

$$X(t) = \sum_{j=1}^{\infty} a_j e^{i\omega_j t}, \tag{2.8}$$

by admitting variable amplitudes and frequencies. Consequently, its main advantage over Fourier expansion is that it accommodates nonlinear and non-stationary data perfectly.

Equation (2.7) enables us to represent the amplitude and the instantaneous frequency as functions of time in a three-dimensional plot, in which the amplitude is contoured on the time-frequency plane. The time-frequency distribution of amplitude is designated as the Hilbert amplitude spectrum or simply Hilbert spectrum, denoted by $H(\omega, t)$.

Having obtain Hilbert spectrum, One will have no difficult to define the marginal spectrum as following:

$$h(\omega) = \int_0^T H(\omega, t)\mathrm{d}t. \tag{2.9}$$

The marginal spectrum offers a measure of total amplitude(or energy) contribution from each frequency value.

3 HHT-Based Signal Period Analysis

To be convenient, we give three definitions first.

Definition 3.1 *Let $x(t)$ be a arbitrary time series and $h(\omega)$ be its marginal spectrum. Then ω_m is called the main frequency of $x(t)$; if $h(\omega_m) \geq h(\omega),\ \forall\omega$.*

Definition 3.2 *Let $X = \{x_j(t) \mid j = 1, 2, \cdots, n\}$, where each $x_j(t)$ is a time series of m data. Then for any frequency f, the main frequency distribution of X at f is defined as the number of those $x_j(t)$ in X whose main frequencies are f.*

Definition 3.3 *Let $x(t)$ be a periodic time series with period T and main frequency f. Then the difference between f and $1/T$ is defined as main frequency shift, denoted by MFS briefly.*

To expose the relation between the main frequency and the period of a signal, let us observe a simple example firstly.

Let $x(t) = sin(2\pi ft), f = 0.01$. Its marginal spectrum is shown in Fig. 1. One has no difficult in seeing the main frequency of $x(t)$ is 0.01 which is precisely the reciprocal of signal period. On the other hand, It is easy to see that the signal energy is mainly concentrated on the main frequency. It is worth noting that the main frequency energy of such a special signal should theoretically be equal to its total energy because it doesn't contain any other frequency components. The difference between theory and reality is completely caused by computation. However, we think the difference will not cause the vital effect on analysis result.

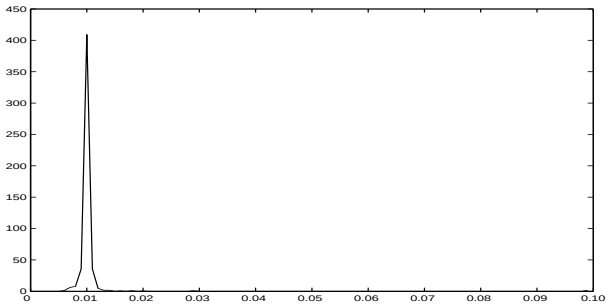

Figure 1: The marginal spectrum of $x(t) = \sin(2\pi ft),\ f = 0.01$

It is unfortunate that most of signals in reality do not like such a special one. They maybe contain various nonlinear distortion. Trying to disclose the affection caused by the signal nonlinearity to main frequency, we give another example as follows.

Let $x(t) = sin(2\pi ft + ksin(2\pi ft)),\ f = 0.01,\ k = 0.1, 0.2, \cdots, 0.9$. Their waveforms which are distorted from the sine waveform can be treated as the results caused by nonlinearity. The larger k is, the sharper the distortion is, such as shown in Fig. 2, in which the left part are the waveforms correspond to $k = 0.1 \sim 0.9$ respectively from top to bottom; the right part shows the relation between the main frequency and k where the horizontal coordinate represents k and the vertical coordinate represents the main frequency. This experiment suggests that the larger k is, the larger the MFS is. In other words, the sharper the signal nonlinearity is, the larger the MFS is.

This example implies that the nonlinearity, which brings plenty of frequency components in signal, will cause main frequency shift (MFS). In other words, it will be unreliable to estimate signal period according to its main frequency. Most similar experiments conducted by us support the observation.

Fig. 3 is a noisy version of Fig. 2. The left are produced by adding white-noise of abundant high frequency components to those shown on the left of Fig. 2. To ensure that the noisy signal is periodic, we construct a segment of white-noise with 100 data firstly, then add the segment to every periods of the signal. The waveforms of the noisy signal are shown on the left of Fig. 3, from top to bottom corresponding to $k = 0.1 \sim 0.9$

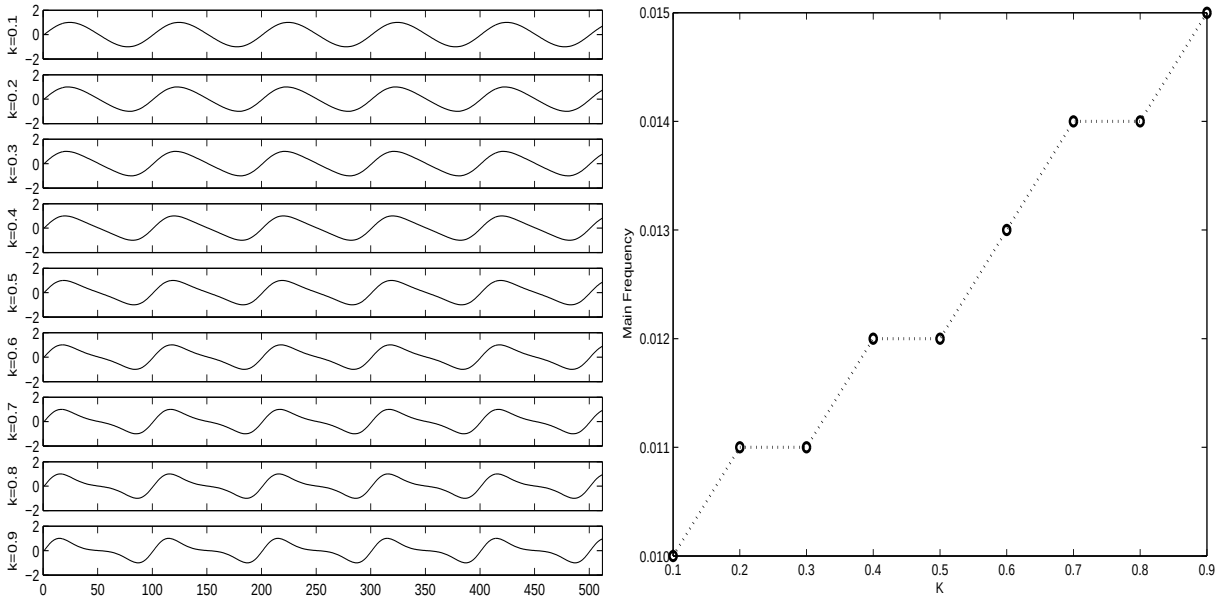

Figure 2: The left part$x(t) = \sin(2\pi ft + 0.1k\sin(2\pi ft))$, $f = 0.01$, the waveforms form top to bottom corresponds to $k = 1, 2, \cdots, 9$ respectively; the right part shows the relation between the main frequency and k.

respectively. Comparing the right of Fig. 3 with the counterparts in Fig.2, it is easy to see that the main frequency shift can be calculated correctly by means of adding white-noise. This interesting observation is supported by a great number of experiments.

It's unfortunate that we fail to interpret theoretically the result now. However, we surely think it mainly profits from the EMD method after a great number of experiments have been conducted, which show that EMD has ability to relieve the nonlinear distortion in low frequency components. When the components whose frequencies are higher than main frequency are abundant enough at each location of a signal, the nonlinearity contained in the main frequency component will be relieved largely, which leads the main frequency shift to be small. As an example, we demonstrate the phenomenon by the 8th signal shown on the left of Fig. 3.

Fig.4 are the 8th signal shown on the left of Fig. 3 (corresponding $k = 0.8$), its 7 imfs and the residue produced by EMD (respectively from top to bottom). It is noticed that the period of 6th imf is about 100, but has much slighter nonlinear distortion than that of the signal shown in 2nd row from bottom on the left of Fig.2. It is well known that EMD extracts frequency components at each location from high frequencies to low frequencies, consequently, the high frequency components, which contaminate a low frequency signal and make the nonlinear distortion, are extracted before the low frequency component is implemented, namely, the nonlinear distortion of the low frequency component is eliminated along with the high frequency extraction.

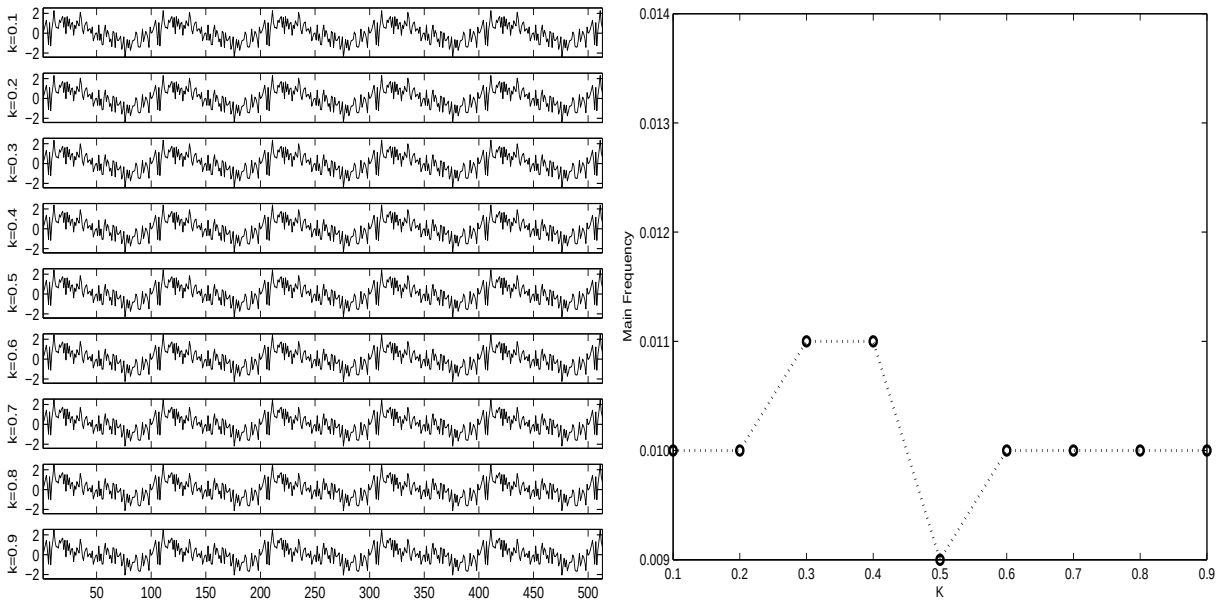

Figure 3: The noisy nonlinear period signals and their main frequency distribution

From the above analysis, it is concluded that the main frequency of a periodic signal which contains enough abundant high frequency components at each location equal approximately to the reciprocal of the signal period.

A great number of experiments have been conducted to verify the conclusion. Fig. 5 shows the distribution with respective to the main frequencies of 100 random periodic signals with period 100 and each containing 300 data. It is easy to see that the main frequencies of the most signals concentrate on about 0.01, which is the reciprocal of 100.

To check the validity of the conclusion for approximately periodic signals, let us consider the following 1000 approximately periodic signals: Firstly, 100 signals each containing 300 data and of amplitude 1 are generated randomly. They are usually nonperiodic signals. Secondly, by adding them to periodic signals $x(t) = k\sin(2\pi ft)$ for $f = 0.01$ and $k = 0, 0.1, \cdots, 0.9$, 1000 signals are constructed. It is easy to see that they are approximately periodic depending on the value of k.

Tab. 1 lists the main frequency distribution corresponding to $k = 0, 0.1, \cdots, 0.9$ from 2nd row to the last row respectively. The maximum of each row is displayed with bold fonts. One has no difficult in seeing that the period can be reliably estimated in most cases, even if the signal has a little periodicity such as the case of $k = 0.1$. Moreover, the higher the periodicity is, the more reliable the estimation is.

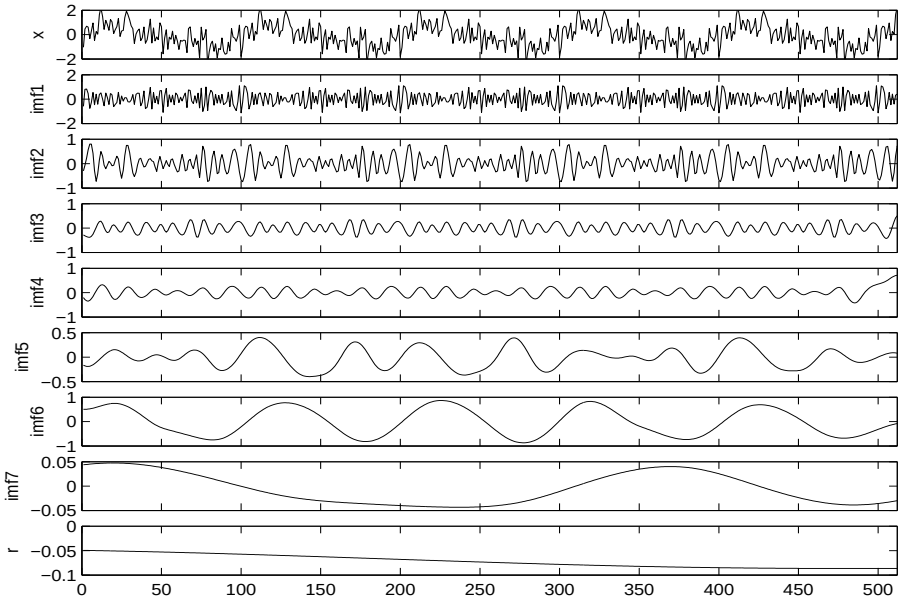

Figure 4: The EMD of $x(t) = \sin(2\pi ft + 0.1k\sin(2\pi ft))$, $f = 0.01$, $k = 0.8$. $x(t)$, its 7 imfs and the residue, are plotted respectively form top to bottom.

4 The Period Analysis of Texture Images

In this section, the analysis and results of Section 3 are employed to estimate the periods of texture images. Before doing this, the simple and classical tactic to divide a two-dimension texture image into one-dimension data, as shown in Fig.6 is used.

After the row or column data are extracted from a texture image, their main frequencies as described in section 3 can be calculate and their main frequency distributions can obtain. Because a natural texture image contains enough abundant high frequency components, it should be reliable to estimate its period along horizontal and/or vertical axes according to the main frequency distributions.

The left of Fig. 7 is a 256×256 texture image D1 from Broadz texture database. It contains about 10 periods along horizontal axis and about 17 periods along vertical axis. The right of Fig. 7 are the main frequency distributions: the top corresponds to the its horizontal data and the bottom corresponds to the vertical data. It is easy to see that the maximum corresponding to the horizontal data is at $f = 0.038 \approx 1/26$. It suggests that its horizontal period can be estimated as about 26, which is close to the real period of 25.6. Similarly, the vertical period can be estimated as about 14.5, which is close to the real period of 15.

The top of Fig. 8 shows the 512×512 texture image D56 from Broadz texture database. To observe how the main frequency distributions change when the textures are similar, we divide it into 4 sub-images of size 256×256 as shown in Fig. 8, in which the 4 sub-images

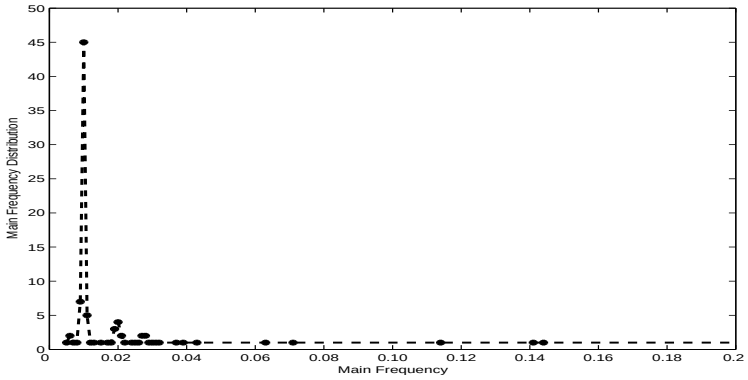

Figure 5: The distribution distribution with respective to the main frequencies of 100 random periodic signals with period 100 and each containing 300 data.

Table 1: The main frequency distribution corresponding to $k = 0, 0.1, \cdots, 0.9$

MF$\times 10^{-3}$	2	3	4	5	6	7	8	9	10	11	12	13	14	15	16	17	others
k=0	1	3	11	11	8	**10**	9	7	3	4	5	2	4		2	3	17
k=0.1			2	7	14	4	11	12	**20**	16	8	2	2			1	
k=0.2	1	2	3	4	5	10	15	20	**22**	10	6	2					
k=0.3		2	3	6	3	3	16	**26**	**26**	11	4						
k=0.4			2	2	1	7	20	**32**	24	11	1						
k=0.5		1	1			2	11	28	**34**	18	5						
k=0.6		2	3		1	2	12	28	**37**	12	3						
k=0.7						2	6	32	**42**	17	1						
k=0.8		1	1			2	5	20	**56**	14	1						
k=0.9			1		1	1	3	29	**50**	15							

are marked with 'A', 'B', 'C' and 'D'. Fig. 8(a), (b), (e) and (f) show their corresponding main frequency distributions along the horizontal axis. It is encouraging to see these main frequency distributions are almost the same. Similarly, Fig. 8(c), (d), (g) and (h) are their main frequency distributions along the vertical axis, which have similar shapes.

The discussion above and a great number of other similar experiments conducted by us summarize that the period of a texture image along some direction can be estimated accurately to a great extent according to its main frequency distribution.

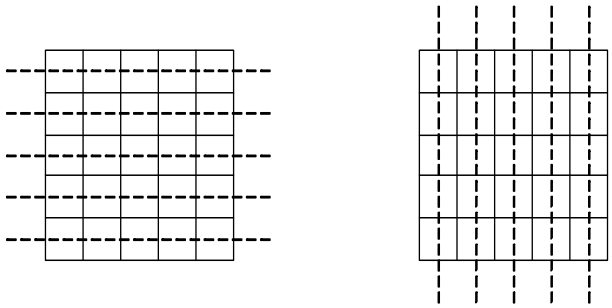

Figure 6: The sketch map of the divide tactic

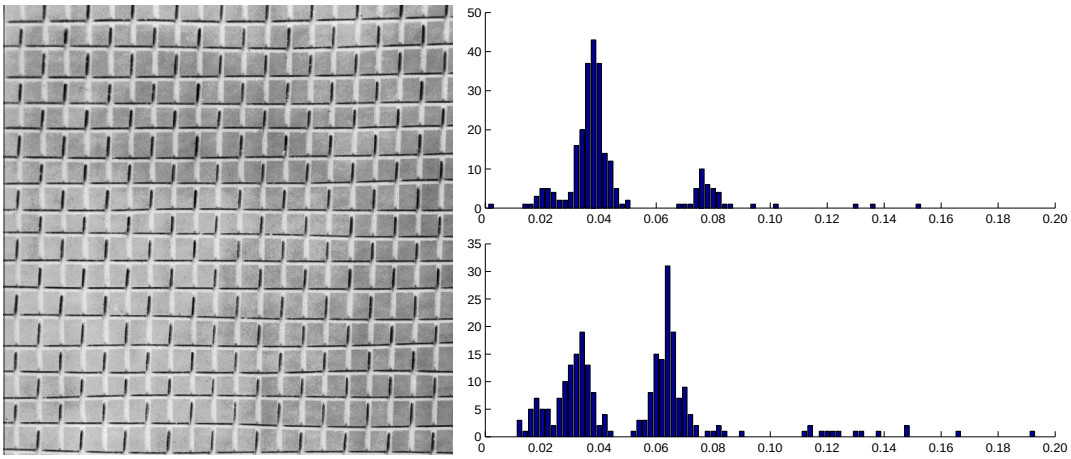

Figure 7: The texture image D1 and its main frequency distribution along horizontal axis

5 Conclusion

This paper gives an approach to analyze period of a signal based on Hilbert-Huang Transform. By analyzing the influence on the main-frequency distribution caused by nonlinearity of the signal, an approximate relation between the period and the main-frequency of an approximately periodic signal which contains plenty of high frequency components is established. Experiments show that one can estimate the period of a signal accurately to a great content according to its main-frequency distribution. This method is robust to noise and can arrive at excellent estimation even if the periodicity of the signal is very weak.

Acknowledgement

The work was done at Sun Yat-sen University, China and Macao University of Science and Technology, Macao. The authors thank their colleagues at these two universities.

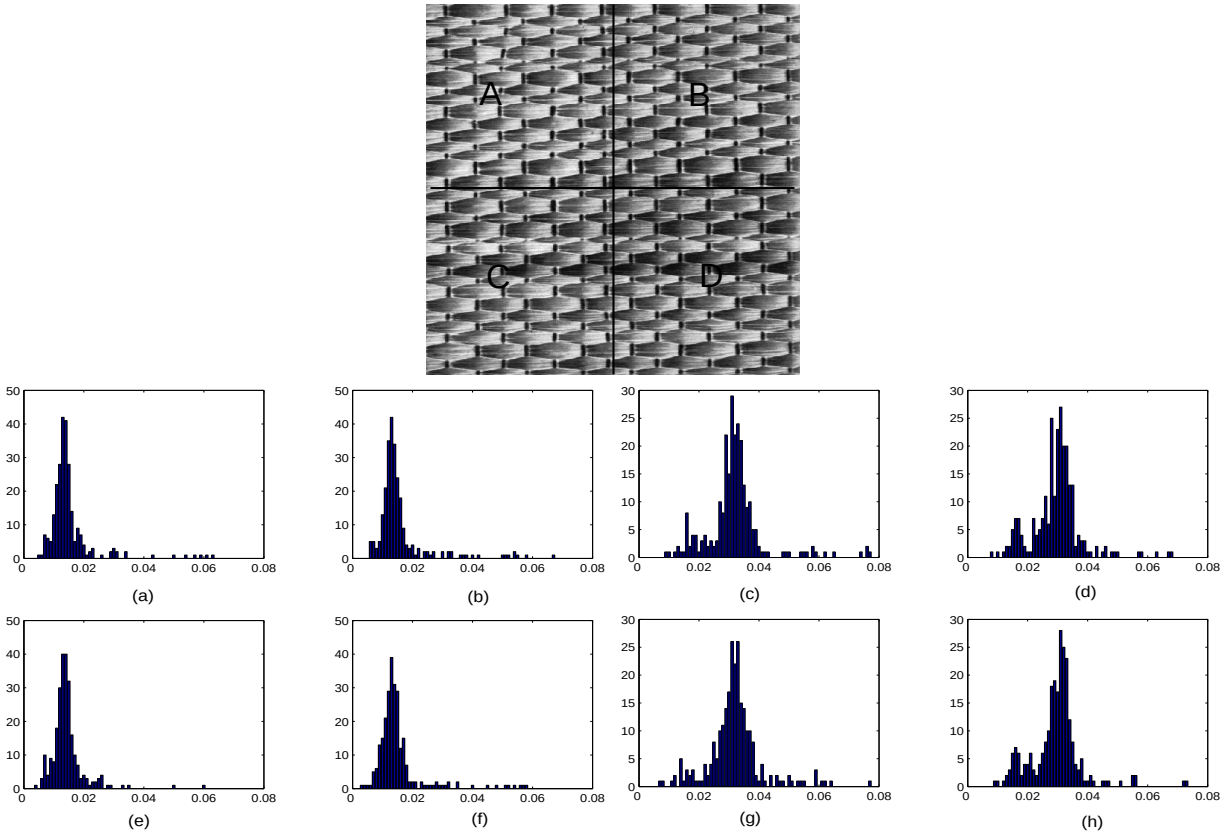

Figure 8: The texture image D56 and the main frequency distributions of its four sub-image in both horizontal and vertical direction

Partial idea of the work was raised while the third author was visiting the Institute for Mathematical Sciences, National University of Singapore in 2003. The visit was supported by the Institute.

References

[1] Hongzhi An and Min Chen. *Non-linear Time series Analysis*. Shanghai Science & Technology Press, China, 1998.

[2] Yongjun Deng, Wei Wang, Chengchun Qian, and Dejun Dai. Boundary-processing-technique in EMD method and Hilbert transform. *Chinese Science Bulletin*, 46(3):954–961, 2001.

[3] P. Flandrin, G. Rilling, and P. Goncalves. Empirical mode decomposition as a filter bank. *IEEE SIGNAL PROCESSING LETTERS*, 11(2):112–114, 2004.

[4] Chunming Han, Huadong Guo, Changlin Wang, Dian Fan, and Huiyong Sang. Multiscale edge detection based on EMD. *High technology letters (Chinese version)*, 6:13–17, 2003.

[5] N. E. Huang, Z. Shen, and S. R. Long et al. The empirical mode decomposition and the Hilbert spectrum for nonlinear and non-stationary time series analysis. *Proc. R. Soc. Lond. A*, pages 903–995, 1998.

[6] N. E. Huang, Z. Shen, and S. R. Long. A new view of nonlinear water waves: the hilbert spectrum. *Ann Rev Fluid Mech*, 31:417–457, 1999.

[7] Wei Huang, Zheng Shen, N. E. Huang, and Yuan Cheng Fung. Engineering analysis of biological variables: An example of blood pressure over 1 day. *Proc. Natl. Acad. Sci. USA*, 95:4816–4821, 1998.

[8] Wei Huang, Zheng Shen, N. E. Huang, and Yuan Cheng Fung. Nonlinear indicial response of complex nonstationary oscillationsas pulmonary hypertension responding to step hypoxia. *Proc. Natl. Acad. Sci. USA*, 96:1834–1839, 1999.

[9] C. H. Loh, T. C. Wu, and N. E. Huang. Application of emd+hht method to identify near-fault ground motion characteristics and structural responses. *BSSA, Special Issue of Chi-Chi Earthquake*, 91(5):1339–1357, 2001.

[10] J. C. Nunes, Y. Bouaoune, E. Delechelle, S. Guyot, and Ph. Bunel. Texture analysis based on the bidimensional empirical mode decomposition. *Machine Vision and Application*, 2003.

[11] J. C. Nunes, Y. Bouaoune, E. Delechelle, O. Niang, and Ph. Bunel. Image analysis by bidimensional empirical mode decomposition. *Image and Vision Computing*, 21:1019–1026, 2003.

[12] S. C. Phillips, R. J. Gledhill, J. W. Essex, and C. M. Edge. Application of the Hilbert-Huang Transform to the analysis of molecular dynamic simulations. *J. Phys. Chem.*, A(107):4869–4876, 2003.

[13] E. C. Titchmarsh. *Introduction to the Theory of Fourier Integrals*. Oxford University Press, 1948.

[14] Zhihua Yang, Dongxu Qi, and Lihua Yang. A novel approch for detecting pitch based on Hilbert-Huang Transform. *Technical Report, Sun Yat-sen University*, 2004.

[15] Zhihua Yang, Dongxu Qi, and Lihua Yang. A novel automated detection of spindles from sleep eegs based on hilbert-huang transform. *Technical Report, Sun Yat-sen University*, 2004.